Modeling of streamer in gas by FEM and semi-Lagrangian method

Amine Bennini, Raphaël Pile, Guillaume Parent

Modeling of Streamer in Gas by FEM and Semi-Lagrangian Method

Amine Bennini[1], Raphaël Pile[2] and Guillaume Parent[1]
[1]Univ. Artois, UR 4025, Laboratoire Systèmes Électrotechniques et Environnement (LSEE), F-62400 Béthune, France
[2]Arts et Métiers Institute of Technology, LISPEN, F-59046 Lille, France

Determining the likelihood of occurrence, growth and extinction of partial discharges between two conductors is a key point when designing electrical devices such as transformers, electrical machines or busbars. The continuity equations governing both time- and position-dependence of charged particle densities makes it possible to build the most comprehensive model of partial discharge development in gas. Known in the literature as fluid model, plasma model or even electrohydrodynamic model, it consists of a set of advection-diffusion-reaction type equations strongly coupled to Poisson's equation that still remains challenging to solve by means of FEM due to numerical instability. This paper deals with the modeling of spatio-temporal growth of partial discharge inside gas using FEM and stabilized by a semi-Lagrangian method. The main contribution lies in the development of the weak formulation of the state problem in the general case for the electro-hydrodynamic problem. The simulation based on this formulation of the POSS method is validated for a streamer discharge.

***Index Terms*—Finite element analysis, partial discharges, conservation equations, Poisson's equation, streamer.**

I. Introduction

In the past decades, power electronics allowed to drastically increase the efficiency of electrical devices but also led to both higher operating voltage and switching frequency which are responsible for partial discharges (PD) appearance in the electrical insulation system of electrical devices. To avoid early aging and thus failure of the latter, the study of PD occurrence in electrical devices recently received considerable attention from designers and researchers. While the ignition, development and extinction mechanism of PD, especially of streamer type, was established in the first half of the previous century [1], [2], efforts in the field of electrical devices focused so far on the determination of the partial discharge inception voltage (PDIV) by means of several empirical criteria such as Paschen's law [3], Schumann's criterion [4] and Raether-Meek's [5], [6] criterion to name a few. Even though those criteria have shown a certain level of usefulness [7]–[11], they are limited when it comes to deeply understand the phenomena involved in partial discharge development.

On the other hand, the continuity equations govern both time- and position-dependence of charged particle densities. When coupled to Poisson's equation, they make it possible to build a comprehensive model of partial discharge development in gas.

First introduced in the 1960s by Davies [12], this approach is referred to as fluid model, plasma model or even electrohydrodynamic model in the literature and is widely used for plasma numerical modeling [12]–[20]. Historically, the finite difference method (FDM) [14] and then the finite volume method (FVM) [15] were used to solve the continuity equations numerically. In the 2000s, Georghiou [16], [17], [21] started to use the FEM to overcome the difficulties encountered by FDM and FVM to deal with complex geometries. Unfortunately, the FEM suffers from numerical instability when it comes to solving advection-diffusion-reaction type equations and requires the use of stabilization methods [22].

Recently, some works on AI-based plasma modeling emerged. Among them, physics-informed neural networks (PINNs), such as the CS-PINN and RK-PINN frameworks proposed by Zhong, have been successfully applied to low-temperature plasmas. These approaches offer mesh-free solutions to drift–diffusion–Poisson systems, underlining the emerging role of AI as a complement to conventional numerical methods [23], [24]. However, AI-based methods have encountered failures when dealing with complex plasma governing equations characterized by variable coefficients and strong non-linearity, according to [25].

In the 2010s, Liu introduced the so-called position-state separation (POSS) method [18], [19] to overcome the numerical instabilities introduced by FEM for convection problems. However, only the diffusive term of the continuity equations were solved by means of FEM in [19] whereas both the ionization the convective acceleration source terms were solved by means of three-order Runge–Kutta method.

This paper aims to solve the whole set of equations, i.e. continuity equations and Poisson's equation, by means of FEM and to derive the appropriate variational formulation for the state sub-problem which was not proposed in [19] and, to the authors' knowledge, is not available in the literature.

The paper is organized in three sections. First, the theoretical background, where both the electrohydrodynamics model and the POSS method are described, is presented in Section II. Then, the variational formulation of the electrohydrodynamics problem stabilized by means of the POSS method, which is the heart of the presented work, is derived in Section III. Finally, that variational formulation is applied to a general advection-diffusion problem test case as well as to a streamer development case in Section IV. As validation, the results are compared to an analytical solution and to numerical results obtained from the literature respectively.

II. Theoretical Background

A. Electrohydrodynamics model

While the ignition, development and extinction mechanism of PD, especially of streamer type, was established in the

first half of the previous century [1], [2], modeling the entire process of its development, from its inception to its (possible) extinction remains a challenge. Up to now, the electrohydrodynamics model [12]–[19] is the most comprehensive model available in the literature that makes it possible to describe the evolution of charge densities in gas, and thus the development of partial discharges, in space and time. It is composed of the continuity equations for electrons, positive and negative ions, which make it possible to account for the development of the space-charge, strongly coupled with Poisson's equation, which allows the modification of the electric field due to that space-charge to be taken into account. It is expressed as [16]:

$$\nabla \cdot (\epsilon \boldsymbol{E}) = e\left(n_{\mathrm{p}} - n_{\mathrm{n}} - n_{\mathrm{e}}\right) \tag{1}$$

$$\begin{aligned}\partial_t n_{\mathrm{e}} = S + (\alpha - \eta) n_{\mathrm{e}} \mu_{\mathrm{e}} \left|\boldsymbol{E}\right| - n_{\mathrm{e}} n_{\mathrm{p}} \beta_{\mathrm{ep}} \\ -\nabla \cdot (n_{\mathrm{e}} \mu_{\mathrm{e}} \boldsymbol{E} - D_{\mathrm{e}} \nabla n_{\mathrm{e}})\end{aligned} \tag{2}$$

$$\begin{aligned}\partial_t n_{\mathrm{p}} = S + n_{\mathrm{e}} \alpha \mu_{\mathrm{e}} \left|\boldsymbol{E}\right| - n_{\mathrm{e}} n_{\mathrm{p}} \beta_{\mathrm{ep}} \\ -n_{\mathrm{n}} n_{\mathrm{p}} \beta_{\mathrm{np}} - \nabla \cdot (n_{\mathrm{p}} \mu_{\mathrm{p}} \boldsymbol{E})\end{aligned} \tag{3}$$

$$\partial_t n_{\mathrm{n}} = n_{\mathrm{e}} \eta \mu_{\mathrm{e}} \left|\boldsymbol{E}\right| - n_{\mathrm{n}} n_{\mathrm{p}} \beta_{\mathrm{np}} - \nabla \cdot (n_{\mathrm{n}} \mu_{\mathrm{n}} \boldsymbol{E}) \tag{4}$$

where t is the time, ϵ is the electric permittivity, $\boldsymbol{E}$ is the electric field, e is the elementary charge, S represents any source/sink mechanism, n_{e}, μ_{e}, n_{p}, μ_{p}, n_{n} and μ_{n} are the charge densities and the mobility for electrons, positive and negative ions respectively and D_{e} is the electron diffusion coefficient. The ionization, attachment, electron–positive-ion recombination and negative-ion–positive-ion recombination coefficients are denoted α, η, β_{ep} and β_{np}.

B. POSS Method

Relations (2), (3) and (4) are all of transport equation type – hyperbolic for (2) and parabolic for (3) and (4) – and can then be expressed under the generic form:

$$\partial_t \rho + \nabla \cdot (\boldsymbol{u}\rho - D\nabla\rho) = s \tag{5}$$

where ρ is the transported quantity, $\boldsymbol{u}$ is the velocity field, D is the diffusion coefficient and s is the source/sink function. The POSS method makes it possible to divide (5) into two sub-problems, called state sub-problem (6) and position sub-problem (7) respectively, by means of operator-splitting [26]:

$$\partial_t \rho = D\Delta\rho - \rho\nabla \cdot \boldsymbol{u} + s \tag{6}$$

$$\partial_t \rho + \boldsymbol{u} \cdot \nabla\rho = 0 \tag{7}$$

Each sub-problem is solved by means of an appropriate method [18]. The state-subproblem (6) deals with the variation of quantity ρ due to diffusive, convective acceleration and source terms. It can partially, as in [18] and [19], or fully be solved by means of FEM on a so-called reference mesh, and the obtained solution is used as the initial condition to solve the position sub-problem (7) at each time step. The position sub-problem, as for it, determines the transport of ρ considering the linear convection only. The method of characteristics [27], applied to (7), makes it possible to compute the transport of quantity ρ by integrating:

$$\partial_t \boldsymbol{x} = \boldsymbol{u}\,. \tag{8}$$

Thus, the convective displacement $\boldsymbol{x}$ of each node of the reference mesh can be computed. It defines a so-called auxiliary transported mesh. The next step is to project the transported ρ from the auxiliary mesh back to the reference mesh. The consecutive solving of each state and position sub-problems is repeated for each time step and for each type of particle (electron, positive ion and negative ion). The process is summarized in Fig. 1.

III. Variational formulation of the state sub-problem

The appropriate variational formulation for the state sub-problem is missing in the corresponding literature. As a consequence, Sections III-A and III-B contain most of the scientific contributions.

A. Mathematical framework

In (6), the classical convective term $\nabla \cdot (\boldsymbol{u}\rho)$ from (5) has been replaced by an unusual convective acceleration term $\rho\nabla \cdot \boldsymbol{u}$. As the weak form of (6) is not found in the scientific literature, the main scientific contribution of this communication is to develop the variational formulation of the state sub-problem. Thus, a Sobolev space H_0^1 with zero values on the boundary is considered. The weak formulation is derived by multiplying the governing equation (6) by a test function $w \in H_0^1(\Omega)$ and integrating over the domain Ω:

$$\int_\Omega \left(\partial_t \rho - D\Delta\rho + \rho\nabla \cdot \boldsymbol{u} - s\right) w \mathrm{d}\boldsymbol{x} = 0, \quad \forall w \in H_0^1\,. \tag{9}$$

Then, applying Green's formula to the diffusive term:

$$\begin{aligned}\int_\Omega \left(w\partial_t\rho + \nabla w \cdot (D\nabla\rho) + w\rho\nabla \cdot \boldsymbol{u} - ws\right) \mathrm{d}\boldsymbol{x} \\ - \int_{\partial\Omega} w(D\nabla\rho) \cdot \mathbf{n} \mathrm{d}s = 0, \quad \forall w \in H_0^1\,.\end{aligned} \tag{10}$$

The boundary term vanishes since $w = 0$ on $\partial\Omega$. Using the scalar product operator $(.,.)$ corresponding to $H_0^1(\Omega)$, the variational formulation problem becomes:

$$(\partial_t\rho, w) + (D\nabla\rho, \nabla w) + (\rho\nabla \cdot \mathbf{u}, w) - (s, w) = 0. \tag{11}$$

Using the following identity:

$$\rho\nabla \cdot \mathbf{u}\, w = \nabla \cdot (\rho w \mathbf{u}) - w\, \mathbf{u} \cdot \nabla\rho - \rho\, \mathbf{u} \cdot \nabla w, \tag{12}$$

the convective acceleration term $(\rho\nabla \cdot \mathbf{u}, w)$ is developed and integrated over Ω:

$$\begin{aligned}\int_\Omega \rho(\nabla \cdot \mathbf{u}) w\, dx = \int_\Omega \nabla \cdot (\rho w \mathbf{u})\, dx \\ - \int_\Omega w\mathbf{u} \cdot \nabla\rho\, dx - \int_\Omega \rho\mathbf{u} \cdot \nabla w\, dx.\end{aligned} \tag{13}$$

Then, the divergence theorem (Gauss' theorem) is applied to the first term on the right-hand side. This transforms the volume integral of the divergence into a surface integral over the boundary $\partial\Omega$:

$$\int_\Omega \nabla \cdot (\rho w \mathbf{u})\, dx = \int_{\partial\Omega} (\rho w \mathbf{u}) \cdot \mathbf{n}\, ds, \tag{14}$$

where $\mathbf{n}$ is the outward-pointing unit normal vector on $\partial\Omega$. Since the test function w belongs to $H_0^1(\Omega)$, it vanishes on the boundary. Consequently, the product $\rho w\mathbf{u}$ is also zero on $\partial\Omega$, and thus the surface integral vanishes:

$$\int_{\partial\Omega} (\rho w\mathbf{u}) \cdot \mathbf{n}\, ds = 0. \tag{15}$$

This simplification eliminates the flux term from the variational expression (13) leading to:

$$(\rho\nabla \cdot \mathbf{u}, w) = -(\mathbf{u} \cdot \nabla\rho, w) - (\rho\mathbf{u}, \nabla w). \tag{16}$$

Replacing the convective acceleration term in equation (11) using (16), the final variational formulation of the state sub-problem (6) is obtained:

$$\begin{aligned}(\partial_t\rho, w) + (D\nabla\rho, \nabla w) - (\boldsymbol{u} \cdot \nabla\rho, w)\\ -(\rho\boldsymbol{u}, \nabla w) - (s, w) = 0.\end{aligned} \tag{17}$$

The rigorous development of (17) reveals two terms: $-(\boldsymbol{u} \cdot \nabla\rho, w)$ and $-(\rho\boldsymbol{u}, \nabla w)$. Only the first term, i.e. $-(\boldsymbol{u} \cdot \nabla\rho, w)$, was found in the POSS Matlab code published as a supplementary file of [18], highlighting the necessity of the proposed mathematical development.

B. Application to electrohydrodynamics model

The variational formulation expressed in (17) provides a consistent framework for solving generic transport equations. However, when applied to the electrohydrodynamics model introduced in II-A, the overall complexity of the problem increases considerably. Each charged species (electrons, positive ions, and negative ions) is governed by a advection-diffusion-reaction equation that fits into the general structure addressed in this formulation. Nevertheless, the presence of strong nonlinearities due to field-dependent ionization, attachment, and recombination rates and the coupling with Poisson's equation for the electric field, introduce additional challenges. As a result, the variational formulation (17) must be applied separately to each transport equation for n_e, n_p, and n_n, while accounting for strong nonlinear couplings between them and with the electric field. This leads to a strongly coupled, nonlinear, and time-dependent system.

The three weak forms corresponding to the state sub-problem equations of each charged species in the fluid model are derived from (17).

Electron state sub-problem formulation:

$$\begin{aligned}(\partial_t n_e, w) + (D_e\nabla n_e, \nabla w) - (\mu_e\mathbf{E} \cdot \nabla n_e, w) - (n_e\mu_e\mathbf{E}, \nabla w)\\ -(S + (\alpha - \eta)n_e\mu_e|\mathbf{E}| - n_e n_p\beta_{ep}, w) = 0, \quad \forall w \in H_0^1.\end{aligned} \tag{18}$$

Positive ion state sub-problem formulation:

$$\begin{aligned}(\partial_t n_p, v) - (\mu_p\mathbf{E} \cdot \nabla n_p, v) - (n_p\mu_p\mathbf{E}, \nabla v)\\ -(S + \alpha n_e\mu_e|\mathbf{E}| - n_n n_p\beta_{np}, v) = 0, \quad \forall v \in H_0^1.\end{aligned} \tag{19}$$

Negative ion state sub-problem formulation:

$$\begin{aligned}(\partial_t n_n, \psi) - (\mu_n\mathbf{E} \cdot \nabla n_n, \psi) - (n_n\mu_n\mathbf{E}, \nabla\psi)\\ -(\eta n_e\mu_e|\mathbf{E}| - n_n n_p\beta_{np}, \psi) = 0, \quad \forall \psi \in H_0^1.\end{aligned} \tag{20}$$

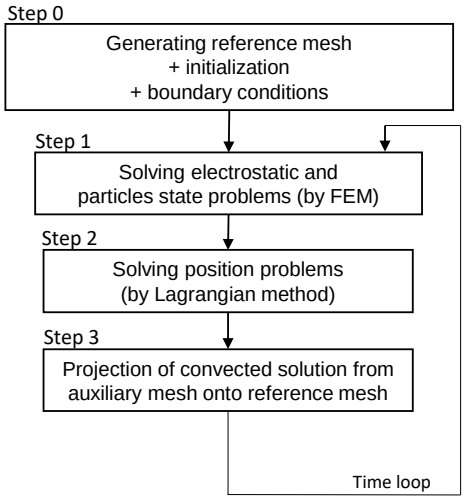

Fig. 1. Solving Process (POSS): Step 0 includes the generation of the reference mesh which is used for the FEM, initialization of unknowns and boundary conditions; Step 1 includes the solving by FEM of electric field (1) and the state problems (18)-(19)-(20); Step 2 includes the solving of position problems (21)-(22)-(23) by a Lagrangian method, which generates auxiliary meshes with a convected solution; Step 3 includes the mesh-to-mesh projection of the convected solution from the auxiliary mesh onto the reference mesh. Steps 1-2-3 are performed for each time step.

Variational problems (18), (19) and (20) are solved by FEM. However, these variational problems need to be associated with their corresponding position problem (solved by Lagrangian method) to fully solve the electrohydrodynamics model:

$$\partial_t\boldsymbol{x}_e = \mu_e\mathbf{E}\,, \tag{21}$$

$$\partial_t\boldsymbol{x}_p = \mu_p\mathbf{E}\,, \tag{22}$$

$$\partial_t\boldsymbol{x}_n = \mu_n\mathbf{E}\,. \tag{23}$$

where $\boldsymbol{x}_e$, $\boldsymbol{x}_p$ and $\boldsymbol{x}_n$ are the nodal displacement fields of each type of particles. These nodal displacements make it possible to to compute a convected auxiliary mesh for each particle (each node of the reference mesh is moved according to the displacement field) [18]. The algorithmic solving process is summarized in Fig. 1. Compared to previous work using semi-Lagrangian method, the convective acceleration term is fully included as in (17) and can be solved by FEM.

IV. Application tests and results

A. General advection-diffusion problem test

A one-dimension advection-diffusion problem of the form of (5) is considered. The diffusion coefficient, convective velocity, and source terms are chosen as $D = (1-x)^2$, $u = 1 - x$, and $f = 0$ respectively. In addition, Dirichlet boundary conditions are applied such that $\rho(0,t) = 1$ and $\rho(1,t) = 0$. Under these assumptions, the exact solution of the problem is given by [27]:

$$\rho(x,t) = \frac{1}{1-x}\,\mathrm{erfc}\left\{\frac{\ln(1-x)}{-2\sqrt{t}}\right\} \tag{24}$$

where $\mathrm{erfc}(\cdot)$ denotes the complementary error function.

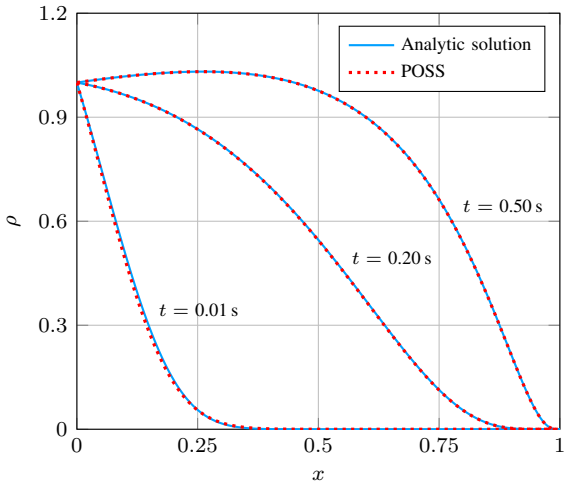

Fig. 2. Comparison between analytical solution given by (24) and the POSS numerical solution of the one-dimensional advection–diffusion equation (5), for different time steps.

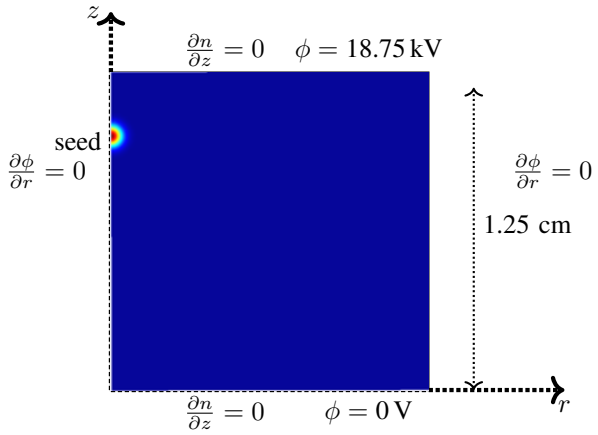

Fig. 3. Two-dimensional axisymmetric representation of a 1.25 cm long air gap with a parallel-plane electrode configuration. A Gaussian seed of positive ions is initially placed at $z = 1\,\mathrm{cm}$. The variables n and ϕ represent the charge densities (either electrons or positive ions) and the electric potential respectively.

The mesh used for the computation is made of 201 nodes (200 edges), evenly distributed along the studied domain, which is fine enough for such a problem, and the time step is set at $\Delta t = 1\,\mathrm{ms}$ in order to fulfill the Courant–Friedrichs–Lewy condition.

Fig. 2 presents a comparison between the analytical solution and the numerical results obtained using the variational formulation of the POSS method presented in Section III, i.e. by fully solving the state-subproblem (6) by means of FEM (see Fig. 1), for this benchmark. As observed in Fig. 2, the numerical solution closely matches the analytical curves since the L^2 norm relative error is 1.97 %, 0.4 % and 0.7 % for $t = 0.01\,\mathrm{s}$, $t = 0.20\,\mathrm{s}$ and $t = 0.50\,\mathrm{s}$ respectively.

B. 2D streamer simulation

In order to facilitate direct comparison between the present simulation results and previously published data, the first benchmark reported in [13] is considered. In this case, only electrons and positive ions are considered. Moreover, no photoionization source (S) nor recombinations between species are considered ($\beta_{\mathrm{ep}} = \beta_{\mathrm{np}} = 0$). Under those assumptions (2), (3) become:

$$\partial_t n_{\mathrm{e}} = (\alpha - \eta) n_{\mathrm{e}} \mu_{\mathrm{e}} |\boldsymbol{E}| - \nabla \cdot (n_{\mathrm{e}} \mu_{\mathrm{e}} \boldsymbol{E} - D_{\mathrm{e}} \nabla n_{\mathrm{e}}) \quad (25)$$

$$\partial_t n_{\mathrm{p}} = (\alpha - \eta) n_{\mathrm{e}} \mu_{\mathrm{e}} |\boldsymbol{E}| \quad (26)$$

while (4) is not considered. In addition, (1) becomes:

$$\nabla \cdot (\epsilon \nabla \phi) = -e\,(n_{\mathrm{p}} - n_{\mathrm{e}}) \quad (27)$$

where ϕ is the electric scalar potential related to the electric field such that $\boldsymbol{E} = -\nabla \phi$.

The computational domain, illustrated in Fig. 3, is an axisymmetric region with both radius $r_{\max}$ and height $z_{\max}$ equal to 1.25 cm. A vertical electrical field is applied by setting the electric potential ϕ such that $\phi\,(z = 0\,\mathrm{mm}) = 0\,\mathrm{V}$ and $\phi\,(z = z_{\max}) = 18.75\,\mathrm{kV}$. As a result, a uniform background electric field of $15\,\mathrm{kV\,cm^{-1}}$ is established within the air gap. Since the initial electric field alone is not sufficient to have the effective ionization in the domain, a Gaussian seed of positive ions is introduced at a height of 1 cm above the cathode.This seed enhances the local electric field, raising it above the dielectric strength of air. The initial distribution of positive ions is prescribed according to (28), representing a Gaussian profile centered at $(r = 0, z = z_0)$:

$$n_p = 10^{13} + 5 \times 10^{18} \exp\left(-\frac{r^2 + (z - z_0)^2}{\sigma^2}\right) \mathrm{m^{-3}} \quad (28)$$

where z and r denote the axial and radial coordinates, respectively, with $z_0 = 10\,\mathrm{mm}$ and $\sigma = 0.4\,\mathrm{mm}$ [13]. Homogeneous Neumann boundary conditions are imposed on all boundaries for both electrons and positive ions densities. The mobility and diffusion coefficients for electrons, the ionization and attachment coefficients values are:

$$\mu_{\mathrm{e}} = 2.3987\,|\boldsymbol{E}|^{-0.26}\,\mathrm{m^2\,V^{-1}\,s^{-1}}$$

$$D_{\mathrm{e}} = 4.3628 \times 10^{-3}\,|\boldsymbol{E}|^{0.22}\,\mathrm{cm^2\,s^{-1}}$$

$$\alpha = (1.1944 \times 10^6 + 4.3666 \times 10^{26}/|\boldsymbol{E}|^3)\mathrm{e}^{-2.73\times10^7/|\boldsymbol{E}|}\mathrm{cm^{-1}}$$

$$\eta = 340.75\,\mathrm{cm^{-1}}$$

The mesh used for this case is composed of 216 542 nodes and 431 330 triangular elements as shown in Fig. 4.

Figs. 5 to 7 present the results obtained by means of POSS (with the variational formulation presented in III-B) according to the procedure described in Fig. 1. In Figs. 6 and 7, CN, FR, TUE, ES, DE and CWI refer to the six different research groups that contributed to [13].

Fig. 5 presents the electric field strength $|\boldsymbol{E}|$ during the propagation of the streamer for different time steps. The results in terms of electric field strength and position of the head of the streamer with respect to time are consistent with the results presented in [13]. In addition, Fig. 6 shows the values of the electric field strength $|\boldsymbol{E}|$ along the axis of symmetry for different time steps. A slight difference from the results obtained by research group CWI in terms of position of the head of the streamer can be noted for $t = 2\,\mathrm{ns}$ and $t = 4\,\mathrm{ns}$.

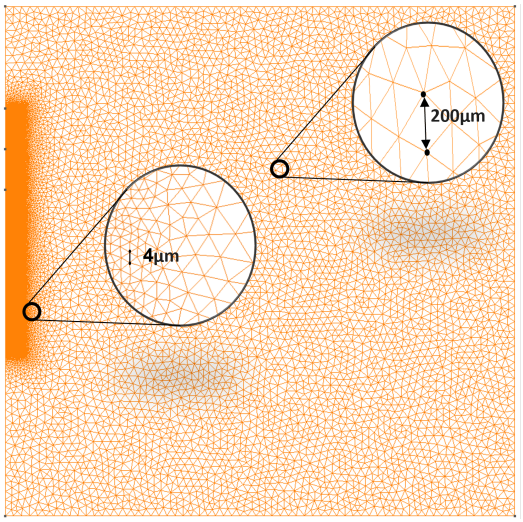

Fig. 4. Meshed geometry. The most finely meshed and coarsely meshed areas are highlighted.

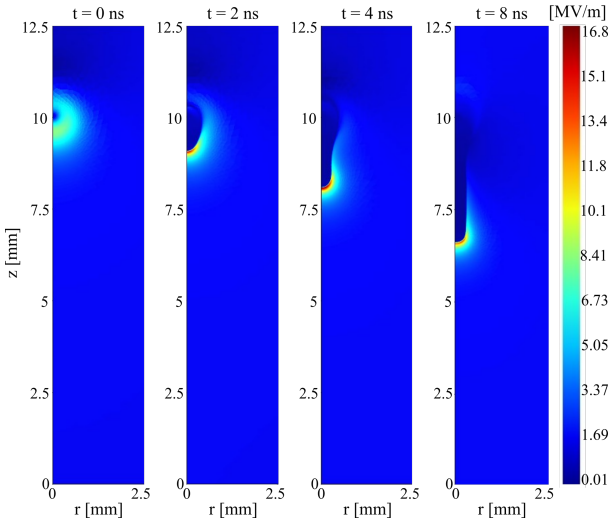

Fig. 5. Electric field strength $|\boldsymbol{E}|$ during the propagation of the streamer inside the studied domain for $t = 0\,\text{ns}$, $t = 2\,\text{ns}$, $t = 4\,\text{ns}$ and $t = 8\,\text{ns}$. The domain shown here is reduced to $r \in [0, 2.5\,\text{mm}]$ for the sake of readability.

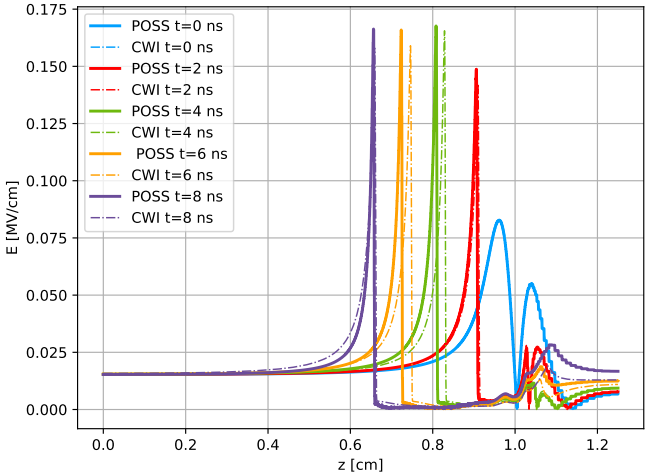

Fig. 6. Electric field strength $|\boldsymbol{E}|$ along the axis of symmetry ($r = 0$) for different time steps. The results obtained by the POSS method are compared to the ones obtained by group CWI [13].

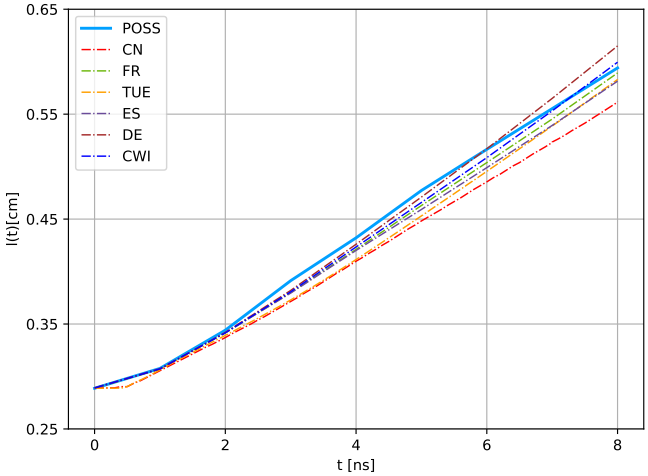

Fig. 7. Value of $l(t)$ (distance between the upper electrode and the head of the streamer) for different time steps. The results obtained by POSS are compared to ones obtained by each of the six research groups involved in [13]

To go one step further on that point, let's note $l(t)$ the distance between the upper electrode, i.e. $z = z_{\text{max}}$, and the position of the head of the streamer, i.e. $z = z(|\boldsymbol{E}|_{\text{max}})$. The value of $l(t)$ for different time steps is presented in Fig. 7 and compared to the results obtained by each of the six aforementioned research groups. Again, the results obtained by means of POSS are consistent with those presented in [13]. It proves that the variational formulation proposed for the convective acceleration term in (17) is stable in the POSS algorithm.

V. Conclusion

This paper presented an approach for modeling the spatio-temporal development of streamers in gas using the Finite Element Method (FEM) stabilized by the Position-State Separation (POSS) method. A key contribution lies in the derivation of the variational formulation for the state sub-problem, which includes the convective acceleration term and enables the full resolution of an electrohydrodynamics model within a FEM framework. The proposed method was validated against an analytical solution for a benchmark advection-diffusion problem. Furthermore, its application to a 2D axisymmetric streamer simulation in air confirmed its capability to capture the dynamics of a streamer propagation, with results similar to other research groups. Future work will focus on extending the model to include additional physical phenomena such as photoionization, as well as adaptive meshing strategies to enhance computational efficiency: given that there is already a mesh-to-mesh projection in the POSS method, the additional cost of an adaptive mesh would, in principle, be limited. However, it will be necessary to confirm the relevance of an adaptive mesh in terms of stability and accuracy.

REFERENCES

[1] L. B. Loeb and J. M. Meek, "The mechanism of spark discharge in air at atmospheric pressure. I," *J. Appl. Phys.*, vol. 11, no. 6, pp. 438–447, Jun. 1940.

[2] ——, "The mechanism of spark discharge in air at atmospheric pressure. II," *J. Appl. Phys.*, vol. 11, no. 7, pp. 459–474, Jul. 1940.

[3] F. Paschen, "Ueber die zum funkenübergang in luft, wasserstoff und kohlensäure bei verschiedenen drucken erforderliche potentialdifferenz," *Annalen der Physik*, vol. 273, no. 5, pp. 69–96, 1889.

[4] W. O. Schumann, "Über das minimum der durchbruchfeldstärke bei kugelelektroden," *Archiv für Elektrotechnik*, vol. 12, no. 6-12, pp. 593–608, Jun. 1923.

[5] H. Raether, "Über den aufbau von gasentladungen. I," *Zeitschrift für Physik*, vol. 117, no. 5-6, pp. 375–398, Mar. 1941.

[6] ——, "Über den aufbau von gasentladungen. II," *Zeitschrift für Physik*, vol. 117, no. 7-8, pp. 524–542, Apr. 1941.

[7] N. Hayakawa and H. Okubo, "Partial discharge characteristics of inverter-fed motor coil samples under AC and surge voltage conditions," *IEEE Electr. Insul. Mag.*, vol. 21, no. 1, pp. 5–10, Jan. 2005.

[8] G. Parent, M. Rossi, S. Duchesne, and P. Dular, "Determination of partial discharge inception voltage and location of partial discharges by means of Paschen's theory and FEM," *IEEE Trans. Magn.*, vol. 55, no. 6, pp. 1–4, Jun. 2019.

[9] T. Mathurin, S. Duchesne, and G. Parent, "Assessment of finite element simulation methodologies for the use of Paschen's law in the prediction of partial discharge risk in electrical windings," *IEEE Access*, vol. 8, pp. 144 557–144 564, Jul. 2020.

[10] L. Lusuardi, "Towards a partial discharge free insulation system for the more electrical transportation," Ph.D. dissertation, University of Bologna, Italy, 2020.

[11] C. Montijn and U. Ebert, "Diffusion correction to the Raether–Meek criterion for the avalanche-to-streamer transition," *J. Phys. D: Appl. Phys.*, vol. 39, no. 14, pp. 2979–2992, Jul. 2006.

[12] A. J. Davies, C. J. Evans, and F. Jones Llewellyn, "Electrical breakdown of gases : the spatio-temporal growth of ionization in fields distorted by space charge," *Proc. Roy. Soc. London. Ser. A. Math. Phys. Sci.*, vol. 281, no. 1385, pp. 164–183, Sep. 1964.

[13] B. Bagheri, J. Teunissen, U. Ebert, M. M. Becker, S. Chen, O. Ducasse, O. Eichwald, D. Loffhagen, A. Luque, D. Mihailova, J. M. Plewa, J. van Dijk, and M. Yousfi, "Comparison of six simulation codes for positive streamers in air," *Plasma Sources Sci. Technol.*, vol. 27, no. 9, p. 095002, Sep. 2018.

[14] A. Davies, C. Evans, P. Townsend, and P. Woodison, "Computation of axial and radial development of discharges between plane parallel electrodes," *Proc. Inst. Electr. Eng.*, vol. 124, no. 2, p. 179, Feb. 1977.

[15] S. K. Dhali and P. F. Williams, "Two-dimensional studies of streamers in gases," *J. Appl. Phys.*, vol. 62, no. 12, pp. 4696–4707, dec 1987.

[16] G. E. Georghiou, R. Morrow, and A. C. Metaxas, "Two-dimensional simulation of streamers using the FE-FCT algorithm," *J. Phys. D: Appl. Phys.*, vol. 33, no. 3, pp. L27–L32, Feb. 2000.

[17] G. E. Georghiou, A. P. Papadakis, R. Morrow, and A. C. Metaxas, "Numerical modelling of atmospheric pressure gas discharges leading to plasma production," *J. Phys. D: Appl. Phys.*, vol. 38, no. 20, pp. R303–R328, Oct. 2005.

[18] L. Liu and M. Becerra, "An efficient semi-Lagrangian algorithm for simulation of corona discharges: The position-state separation method," *IEEE Trans. Plasma Sci.*, vol. 44, no. 11, pp. 2822–2831, Nov. 2016.

[19] ——, "Application of the position-state separation method to simulate streamer discharges in arbitrary geometries," *IEEE Trans. Plasma Sci.*, vol. 45, no. 4, pp. 594–602, Apr. 2017.

[20] H. Jayasinghe, L. Arevalo, R. Morrow, and V. Cooray, "Modeling streamer discharge in air using implicit and explicit finite difference methods with flux correction," *Plasma*, vol. 8, no. 2, p. 21, May 2025.

[21] L. Papageorghiou, A. C. Metaxas, and G. E. Georghiou, "Three-dimensional numerical modelling of gas discharges at atmospheric pressure incorporating photoionization phenomena," *Journal of Physics D: Applied Physics*, vol. 44, no. 4, p. 045203, Feb. 2011.

[22] D. Kuzmin, "A guide to numerical methods for transport equations," Fiedrich-Alexander-Universität, Erlangen-N¨remberg, Tech. Rep., 2010.

[23] L. Zhong, B. Wu, and Y. Wang, "Low-temperature plasma simulation based on physics-informed neural networks: frameworks and preliminary applications," *Physics of Fluids*, vol. 34, no. 8, 2022.

[24] C. Peng, R. V. Sabariego, X. Dong, and J. Ruan, "Numerical simulation of streamer discharge using physics-informed neural networks," *IEEE Trans. Magn.*, vol. 60, no. 3, pp. 1–4, Mar. 2024.

[25] Y. Wang and L. Zhong, "Nas-pinnv2: Improved neural architecture search framework for physics-informed neural networks in low-temperature plasma simulation," *arXiv preprint arXiv:2501.15160*, 2025.

[26] G. Marchuk, "Splitting and alternating direction methods," in *Hanbook of Numerical Analysis*. Elsevier, 1990, vol. 1, pp. 197–462.

[27] A. Kumar, D. K. Jaiswal, and N. Kumar, "Analytical solutions to one-dimensional advection–diffusion equation with variable coefficients in semi-infinite media," *J. Hydrol.*, vol. 380, no. 3, pp. 330–337, 2010.